



TU/E MECHANICAL ENGINEERING  
CONTROL SYSTEMS TECHNOLOGY

**Optimization of the TURTLE's acceleration**

BACHELOR END PROJECT



Author Luuk Poort  
Supervisor dr.ir. M.J.G. van de Molengraft  
Coordinator M.E. van 't Klooster

0902347

Eindhoven, July 1, 2017

# Contents

<b>List of symbols</b>	<b>3</b>
<b>Introduction</b>	<b>4</b>
<b>1 Theory</b>	<b>5</b>
1.1 Wheel dynamics and slip . . . . .	5
1.2 Dynamical equilibrium . . . . .	6
<b>2 Hardware</b>	<b>8</b>
<b>3 Model</b>	<b>9</b>
3.1 Structure . . . . .	9
3.2 Model results . . . . .	10
3.3 Model analysis . . . . .	11
<b>4 Validation</b>	<b>14</b>
4.1 Slip detection . . . . .	14
4.2 Data acquisition . . . . .	14
4.3 Data analysis . . . . .	15
4.4 Slip occurrences . . . . .	16
4.5 Comparison to model . . . . .	17
<b>5 Conclusion</b>	<b>19</b>
<b>6 Discussion</b>	<b>20</b>
6.1 Recommendations . . . . .	21
<b>References</b>	<b>22</b>
<b>Appendices</b>	<b>23</b>
A Centre of gravity influence . . . . .	23
A.1 Varying the height of the COG . . . . .	23
A.2 Varying the x-position of the COG . . . . .	24
A.3 Varying the y-position of the COG . . . . .	25
B Mass influence . . . . .	27
C Moment of inertia influence . . . . .	28

## List of Symbols

Variable	Unit	Description
$\alpha$	$rad/s^2$	The angular acceleration of the TURTLE
$\lambda$	–	The amount of slip of a wheel
$\psi$	$^\circ$	The angle of acceleration of the TURTLE
$\omega_w$	$rad/s$	The rotational speed of a wheel of the TURTLE
$a$	$m/s^2$	The linear acceleration of the TURTLE
$h_G$	$mm$	The height of the centre of gravity of the TURTLE
$I_{zz}$	$kg\ m^2$	Moment of inertia of the TURTLE around its z-axis
$k$	$rad/m$	The trajectory dependent constant which correlates $\alpha$ to $a$ : $\alpha = k a$
$\mu$	–	The friction factor of the wheels of the TURTLE
$m$	$kg$	Mass of the TURTLE
$r_w$	$mm$	The radius of a wheel of the TURTLE
$v_w$	$m/s$	The translational speed of a wheel of the TURTLE
$\vec{g}$	$m/s^2$	The gravitational acceleration
$\vec{n}_a$	–	The direction of acceleration of the TURTLE
$\vec{F}_a$	$N$	The acceleration force
$\vec{F}_n$	$N$	The normal force
$\vec{F}_A$	$N$	The force on wheel A
$\vec{F}_B$	$N$	The force on wheel B
$\vec{F}_C$	$N$	The force on wheel C
$\vec{A}^G$	$mm$	Vector from the centre of gravity to wheel A
$\vec{B}^G$	$mm$	Vector from the centre of gravity to wheel B
$\vec{C}^G$	$mm$	Vector from the centre of gravity to wheel C
$\vec{A}^0$	$mm$	Vector from the origin to wheel A
$\vec{B}^0$	$mm$	Vector from the origin to wheel B
$\vec{C}^0$	$mm$	Vector from the origin to wheel C

## Introduction

Tech United is a team of students and engineers at the Eindhoven University of Technology. [1] The team participates in the Middle Size League (MSL) of RoboCup, an organisation which organizes several robot soccer competitions every year. In the MSL competition, these fully autonomous robots play five versus five and compete for the world championship. The ultimate goal of RoboCup is for a team of fully autonomous humanoid robots to win a match of soccer against the current world champion soccer team by 2050.[2]

The soccer robot of Tech United is called a Tech United RoboCup Team Limited Edition (TURTLE) and is continuously improved to keep competing with the other teams. The Tech United MSL team is the current world champion and aims to remain so. Although the TURTLES are already top of the class, they are less agile than other robots in the competition. To improve the agility, this research is done into the acceleration of the TURTLES. The TURTLES drive fully autonomous and accelerate with a predefined maximum acceleration. It is this predefined maximum acceleration that should be optimized in order to improve the agility of the robots.

## Problem definition

The maximum acceleration of the TURTLE is currently too low. It is limited by slipping of the wheels and by complete tipping of the TURTLE, where one wheel loses contact with the ground. Currently, no efforts are made to model the maximum achievable acceleration. Therefore, the parameters influencing the acceleration are still unknown. This problem results in the following research question and sub-questions:

*How can the acceleration of the TURTLES be improved?*

- 1. What parameters influence the acceleration of the TURTLE and how?*
- 2. What are the current values of these influencing parameters?*
- 3. In what way can these parameters be changed to improve acceleration?*
- 4. Can the TURTLE's acceleration be made dependent on its current state?*

## Summary

In the report, the maximum acceleration of a TURTLE is determined through analytical modelling. This model uses force and moment equilibria to determine both linear and angular acceleration. To obtain the inertial properties, the TURTLE's hardware is evaluated using 3D modelling. After analysis of the model's results, an attempt is made to validate the model with experimental data. Although the validation has not succeeded entirely, conclusions about the model are drawn nonetheless. Finally, the process is discussed and recommendations are made.

# 1 Theory

In this chapter the mechanics of the TURTLE and its dynamic slip behaviour are described. The first section covers the wheel dynamics and the concept of slip. Next, the dynamics of the entire TURTLE is evaluated in order to derive a theoretical model for the maximum acceleration.

## 1.1 Wheel dynamics and slip

During the acceleration of the TURTLE, the wheels must not slip. The TURTLE's drive motors apply a torque on the wheels, which in turn apply a horizontal force on the ground. This is visualized in Figure 1.1.

The acceleration is determined by the acceleration force  $\vec{F}_a = m \vec{a}$ , which is the negative of the inertial force  $\vec{F}_{in} = -m \vec{a}$ . This acceleration is equal to the external horizontally applied friction force  $\vec{F}_f$ , which originates from the applied moment  $\vec{M}$ . If the absolute value of the friction force  $F_f$  exceeds a certain maximum, the wheel surface will slip relative to the ground. This maximum value depends on the friction factor  $\mu$  and the normal force  $F_n$  [3]. The relation describing the occurrence of slip is stated in Equation 1.1 and will be referred to as the *slip condition*.

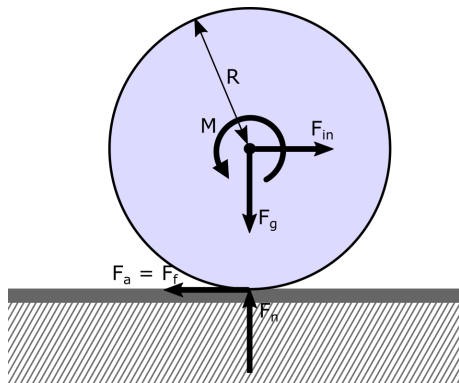


Figure 1.1: Forces on a wheel during acceleration.

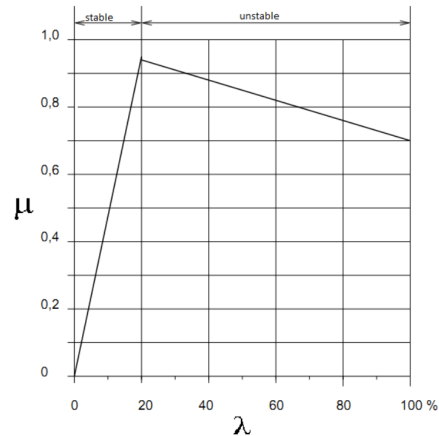


Figure 1.2: The friction factor as a function of the amount of slip.

$$F_a \geq \mu F_n \quad (1.1)$$

$$\lambda = \frac{v_{wheel} - \omega_{wheel} r_{wheel}}{v_{wheel}} \quad (1.2)$$

In this report, the friction factor is modelled as a constant and slip only occurs when the maximum frictional force is exceeded. In reality, a small amount of slip is always present while rolling and the friction factor depends on the amount of slip. The definition of this actual slip is as presented in Equation 1.2. Note that  $v_{wheel}$  is the translational speed of the wheel relative to the ground. At a certain amount of slip, the slip becomes unstable. At this point the friction factor becomes negatively dependent on the slip as visualized in Figure 1.2 [4].

## 1.2 Dynamical equilibrium

To determine the maximum acceleration, the force distribution over the wheels should be such that one wheel is on the verge of slipping. From the slip condition (Equation 1.1), it can easily be seen that the maximum acceleration exists when  $F_a = \mu F_n$ . It is necessary to first determine the forces on each of the wheels, labelled  $A$ ,  $B$ ,  $C$ , before checking them for slip with the slip condition. Aside from the forces on the wheels, the maximal linear and angular acceleration should of course also be determined.

Thus, the unknown variables are:

- $\vec{F}_A$  The force vector of wheel A
- $\vec{F}_B$  The force vector of wheel B
- $\vec{F}_C$  The force vector of wheel C
- $a$  The maximal linear acceleration
- $\alpha$  The maximal angular acceleration

Which comes down to a total of 11 variables. Thus, a minimum of 11 equations are needed to solve the system. This set of equations can be deduced through the evaluation of the dynamical system as done below. These equations follow the convention as shown in Figure 1.3.

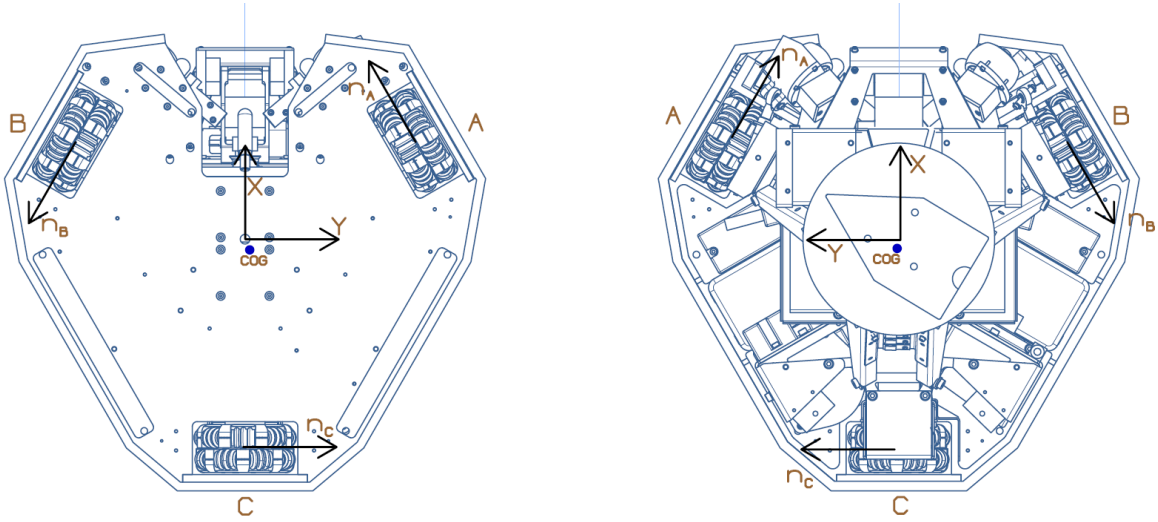


Figure 1.3: Schematic representation of a TURTLE with defined vectors.

The force applied on each of the wheels, consists of the normal force and the acceleration force as seen in Figure 1.1. All three normal forces equal the negative of gravitational force on the TURTLE. All three acceleration forces equal the total acceleration force on the TURTLE. This equilibrium is shown in Equation 1.3a.[3]

Next to the force equilibrium, a moment equilibrium exists around the centre of gravity (COG) of the TURTLE. To incorporate the tipping of the TURTLE as well, it is assumed that the normal forces are all larger than zero. This way, all three wheels remain in contact with the ground, preventing tipping. The only remaining permitted rotation is around the z-axis. The moment equilibrium is given in Equation 1.3b.

The omnivheels of the TURTLE can only deliver a force in their drive direction (see Figure 1.3). The acceleration component of each wheel force can thus be split in its absolute value and its known drive direction: Equation 1.3c.

At maximum acceleration, one of the wheels is on the verge of slipping. The slip condition can be rewritten for all three wheels, such that the maximum over all three equals the friction factor as is done in Equation 1.3d.

Finally, the angular acceleration is assumed to be a function of the linear acceleration. The relation between them is determined from the trajectory the TURTLE is following. For small enough time intervals, the relation can be assumed linear as is done in Equation 1.3e [5].

$$3 \text{ eq. } \rightarrow \quad m a \vec{n}_a - m \vec{g} = \vec{F}_A + \vec{F}_B + \vec{F}_C \quad (1.3a)$$

$$3 \text{ eq. } \rightarrow \quad I_{zz} \alpha \vec{n}_z = \vec{A}^G \times \vec{F}_A + \vec{B}^G \times \vec{F}_B + \vec{C}^G \times \vec{F}_C \quad (1.3b)$$

$$3 \text{ eq. } \rightarrow \quad \begin{bmatrix} F_{i,x} \\ F_{i,y} \\ 0 \end{bmatrix} = \vec{n}_i \left\| \begin{bmatrix} F_{i,x} \\ F_{i,y} \\ 0 \end{bmatrix} \right\| = F_{a,i} \vec{n}_i \quad \text{with } i = A, B, C \quad (1.3c)$$

$$1 \text{ eq. } \rightarrow \quad \mu = \max_{i=A,B,C} \left( \left| \frac{F_{a,i}}{F_{n,i}} \right| \right) \quad (1.3d)$$

$$1 \text{ eq. } \rightarrow \quad \alpha = f(a) = k a \quad (1.3e)$$

Where:

- $m$  The mass of the TURTLE
- $\vec{n}_a$  The direction of acceleration of the TURTLE:  $[\cos(\psi), \sin(\psi), 0]^T$
- $\vec{g}$  The gravitational acceleration:  $-9.81 \vec{e}_z \text{ m/s}^2$
- $I_{zz}$  The moment of inertia of the TURTLE around the z-axis
- $\vec{A}^G$  The vector from the centre of gravity  $G$  to wheel A (analogous for B and C)
- $\vec{n}_i$  The horizontal drive directions of wheels A, B and C (Figure 1.3)
- $\mu$  The friction factor of the wheels
- $k$  The trajectory dependant constant which correlates  $\alpha$  with  $a$

## 2 Hardware

In Chapter 1 it was found that the inertial properties of the TURTLE are needed to determine the maximum acceleration. The TURTLE soccer robot is a complicated robot with dozens of parts. To determine the mass, the centre of gravity and rotational inertias of the TURTLE, a 3D model was evaluated. This model, made in AutoDesk Inventor, allowed the assignment of the component densities. For complex components without clear densities, such as the on-board computer, the components were weighted. From their mass, the corresponding densities were calculated which were then assigned to the 3D modelled part. This method intrinsically assumes that the densities of these complex components are equal over its volume. The measured masses of the components can be found in Table 2.1. The other components had clear or prescribed densities, such as the aluminium frames and the collection of bolts. Note that the last two items of Table 2.1 were not available for measurement and were estimated.

Table 2.1: Masses of components.

<b>Component</b>	<b>Mass (kg)</b>
PC	1.757
Beckhoff Module	1.238
RE25_20W_24V	0.357
Camera (incl. lens)	0.149
RE40_150W_24V	0.838
Housing	1.490
Kinect II	0.619
Kinect Printbox	0.2
Picture Housing	0.3

Having set densities to all components of the model, the AutoDesk Inventor software provided the COG and the inertias of the TURTLE. These properties are displayed in Table 2.2. For the position of the COG, the coordinate frame of Figure 1.3 is used.

Table 2.2: Properties of the TURTLE as determined from the 3D model.

<b>Properties</b>	<b>Value</b>
$m$ [kg]	36.0
$I_{zz}$ [kg m <sup>2</sup> ]	0.799
COG [mm]	$[-3.46, 1.85, 165.59]^T$
$\vec{A}^0$ [mm]	$[97.12, 168.23, 0]^T$
$\vec{B}^0$ [mm]	$[96.63, -167.36, 0]^T$
$\vec{C}^0$ [mm]	$[-206.25, 0, 0]^T$

The properties of the model seem quite accurate as the mass corresponds to the actual TURTLE. Possible errors in the TURTLE's properties will not result in completely unreliable results. In Chapter 3 and Appendix A & B, it is shown that the position of the centre of gravity and the mass of the TURTLE have a small influence on the maximum acceleration.

### 3 Model

In this chapter the model is discussed which calculates the maximum angular and linear acceleration. Firstly, the structure is shortly introduced. Next, results of the model are presented, which are then analysed and discussed.

#### 3.1 Structure

In an effort to model the maximal acceleration of the TURTLE, the theory as discussed in Chapter 1 is implemented in Matlab 2017a. Equation set 1.3 has no distinct value for the direction of acceleration  $\vec{n}_a$ , the friction factor  $\mu$  and the trajectory dependent constant  $k$ . To obtain a simpler implementation, the model is set up in such a way that it solves the maximum acceleration with these undefined parameters as an input. As a particular interest was conveyed by the Tech United team, the height of the centre of gravity was also kept as an input parameter to clearly see its influence on the maximum acceleration. All in all, the model can be represented by the schematic overview as in Figure 3.1.

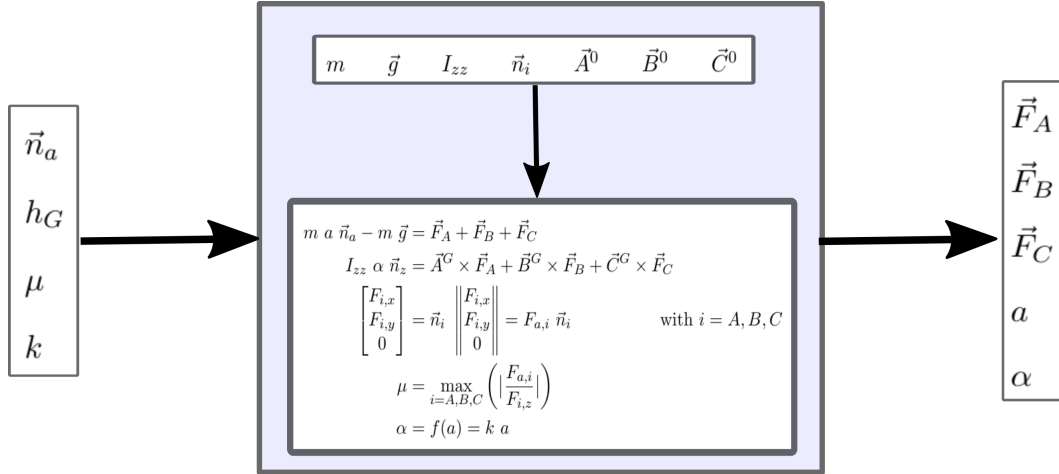


Figure 3.1: Schematic representation of the model.

In Equation 1.3d, the maximum is taken over all three wheels, but the forces are not known initially, so it is unclear to which wheel the equation should be applied. To this end, an assumption is made on the wheel that slips. This is done three times, once for each wheel, to obtain all solutions. The results are compared afterwards to determine the maximum acceleration before slip. Solving the set of equations this way means the results also clearly show the maximum acceleration per wheel as will be seen in Section 3.3.

### 3.2 Model results

In this section, some results from the model are displayed. The maximum acceleration is displayed in the plots as the radius in  $ms^{-2}$  ( $rads^{-2}$  for angular). The angle of acceleration is displayed by the angle in the polar plot. An angle of 0 degrees indicates that the TURTLE is accelerating straight forward. For more results, see the appendices.

**Linear acceleration:**  $\alpha = f(a) = 0$

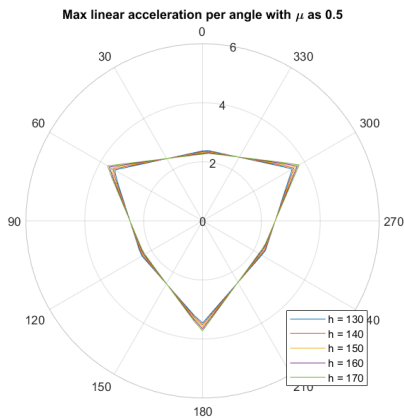


Figure 3.2: Maximum acceleration per angle for different heights of the COG with a friction factor of 0.5.

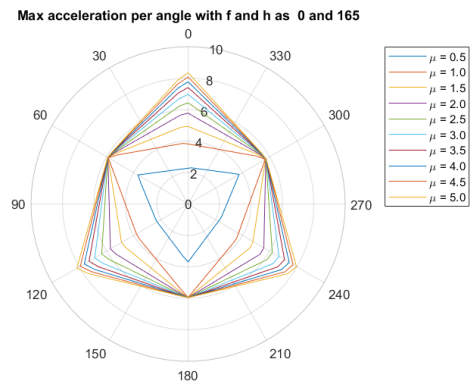


Figure 3.3: Maximum acceleration per angle for different friction factors with a height of the COG of 165 mm.

**Linear and angular acceleration:**  $\alpha = f(a) = k a$

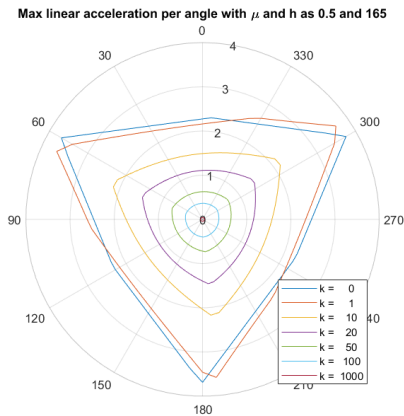


Figure 3.4: Maximum linear acceleration per angle for different factors for  $k$  in  $f = k a$  with a friction factor of 0.5.

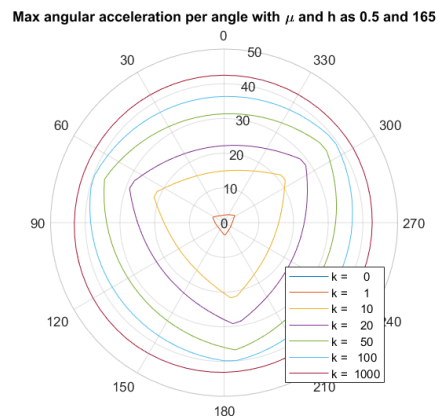


Figure 3.5: Maximum angular acceleration per angle for different factors for  $k$  in  $f = k a$  with a friction factor of 0.5.

### 3.3 Model analysis

In this section the model is analysed. Most noticeable features of the results are discussed and evaluated logically.

- The linear acceleration as displayed in Figure 3.2 is almost symmetrical over three symmetry axes, which is as expected. The results are not completely symmetrical as the force arms of each wheel to the COG are not equal (Chapter 2), which results in slightly different momentums.
- The height of the centre of gravity, as indicated by the multiple lines in Figure 3.2, has an insignificant influence on the maximum acceleration. Although hardly visible, the model shows that for the angles  $-30^\circ$  till  $30^\circ$ , the height of the COG has a small negative influence on the maximum acceleration, while it shows a positive influence for the angles  $30^\circ$  till  $90^\circ$ . Other angles and their influences are shown in Table 3.1. In the angles with a negative relation (e.g.  $\psi = 0$ , driving forward), the front wheels are slipping. Similarly, the rear wheels are slipping in the angles with a positive relation (e.g.  $\psi = 60$ ). When increasing the height of the COG, the arm and therefore the moment of the acceleration forces of the wheels is increased. This is compensated for by increased normal forces on the rear wheels and decreased normal forces of the front wheels. Therefore, a positive influence is observed at slipping back wheels and a negative influence is observed at slipping front wheels.

Table 3.1: Influences of the height of the centre of gravity on the maximum acceleration, depending on the angle of acceleration.

Angle range	Influence of height on acceleration
$-30 < \psi < 30$	negative
$30 < \psi < 90$	positive
$90 < \psi < 150$	negative
$150 < \psi < 210$	positive
$210 < \psi < 270$	negative
$270 < \psi < 330$	positive

- The angle in which the TURTLE accelerates has a big influence on the maximum acceleration possible. In Figure 3.6, the optima in the maximum acceleration are clearly visible. Note that this figure visualises similar data as Figure 3.2. The optima at  $\psi = 60 + c \cdot 120$  with  $c = 0, 1, 2$  belong to the TURTLE accelerating with one wheel in exactly in front and two behind. In this position, the acceleration force is spread evenly over the back wheels which have relatively high normal forces which results in a high maximum acceleration. The optima at  $\psi = c \cdot 120$  with  $c = 0, 1, 2$  arise through the evenly spread forces over the two front wheels. Although this is better than having a single wheel delivering a large force, which is the case at the minima, it is less optimal than having two wheels in the back.
- From Figure 3.7 one can conclude that also the maximum accelerations per wheel are symmetrical over three axes. For specific angles, a certain wheel will never slip, which is visualised by a maximum acceleration of  $0 \text{ m/s}^2$ . Furthermore, there seem to be linear

relations between the angle and the maximum acceleration in the polar plot. If this relation can be determined, this will greatly decrease computation time. A straight line follows  $y = C_1 x + C_2$  with  $x = a \cos \psi$  and  $y = a \sin \psi$ . This means the equation of the maximum acceleration is in the form of Equation 3.1. Note that at the maxima of the curves per wheel (300 ° at A and 60 ° at B) a small irregularity is visible. This irregularity occurs because of the step-size in angle which was used for the model.

$$a = \frac{C_2}{\sin \psi - C_1 \cos \psi} \quad (3.1)$$

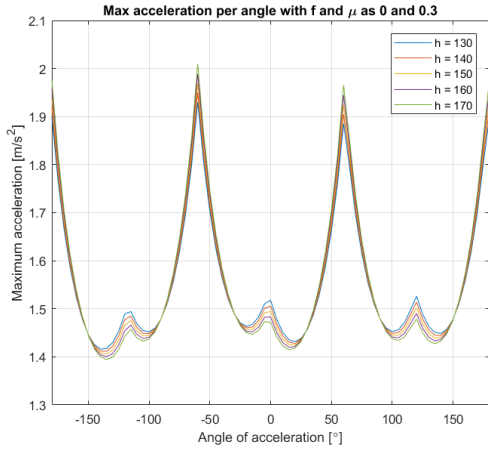


Figure 3.6: Maximum acceleration per angle for different heights of the COG with a friction factor of 0.3.

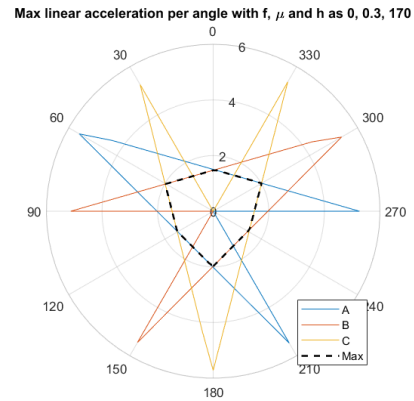


Figure 3.7: Maximum acceleration per angle for each wheel separately and the total maximum acceleration with a friction factor of 0.3 and a height of 165 mm.

- From Figure 3.3, it is obvious that the maximum acceleration has a significant positive relation with friction factor. It can also be concluded that tipping becomes an issue at higher friction factors ( $\mu \geq 1.0$  in Figure 3.3). This can be seen from the limits for the acceleration, which are independent of the friction factor. As previously mentioned in Chapter 1, tipping is incorporated in the model by assuming that the normal forces should be positive. Especially when accelerating with one wheel in the front, tipping becomes an issue due to the relatively small moment the back wheels can exert.
- As shown in Figure 3.4, the maximum linear acceleration decreases with an increase of the factor  $k$  in  $\alpha = f(a) = k a$ . Of course this is logical as more force is applied to accelerate angularly. This is clearly visible in Figure 3.5, which shows that the angular acceleration increases greatly with  $k$ .
- The previously mentioned symmetry of the linear model still appears in the model including rotations as shown in Figure 3.4. However, the symmetry axes shift by a certain rotation which does not seem to have a clear dependency on the value of  $k$ . From Figures 3.8 and 3.9, it can be seen that the angle does shift greatly. With negative

values of  $k$  in  $\alpha = f(a) = k a$ , this angle becomes negative as well, as expected. Note the symmetry around each wheel axis between the two figures, e.g.: the yellow line, belonging to wheel C slipping is mirrored around  $\psi = 0$  when  $k$  changes sign.

- At the pure linear acceleration, a linear relation was observed for the maximum acceleration per wheel. With both linear and angular acceleration, another interesting relation can be found as seen in Figures 3.8 and 3.9. Further study is necessary for determining these relations.

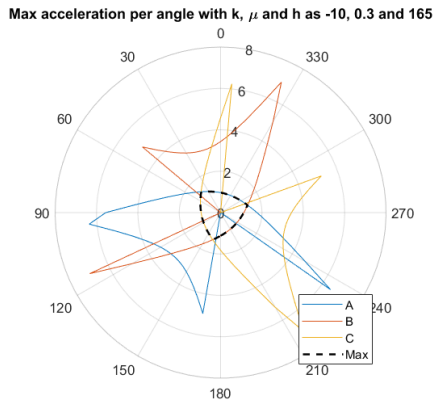


Figure 3.8: Maximum acceleration per angle for each wheel separately and the total maximum acceleration with a friction factor of 0.3, a height of 165 mm and  $k = -10$ .

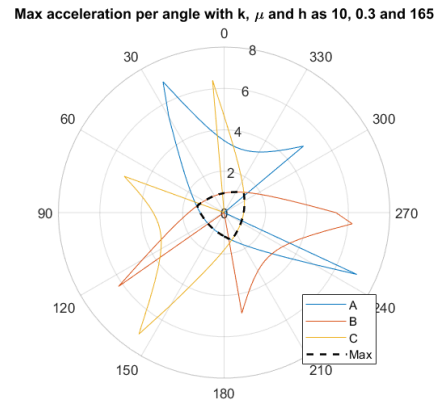


Figure 3.9: Maximum acceleration per angle for each wheel separately and the total maximum acceleration with a friction factor of 0.3, a height of 165 mm and  $k = 10$ .

- As can be seen from Figures 3.4 and 3.5, the maximum acceleration becomes independent of the angle of acceleration at large values of  $k$ . Clearly, this occurs due to the fact that the linear acceleration becomes negligibly small compared to the angular acceleration. The angular acceleration is independent of the angle of acceleration and is now the limiting factor. Assessing the solution of  $k = 1000$  in Figure 3.5, the maximum acceleration converges to a perfect circle as expected. Pure angular acceleration is still dependent on the friction factor (Appendix C). Accelerating only angularly might be the easiest way for determining the friction factor of the wheels.

## 4 Validation

### 4.1 Slip detection

To validate the model as presented in the previous chapter, measurements were done on the actual TURTLES. Due to time constraints the validation was only applied to purely linear accelerations. Incorporation of angular acceleration requires a vast amount of measurements. Using manual mode, the TURTLE was accelerated in all direction with 10 degree intervals and with accelerations ranging from 1.8 to 3.6  $m/s^2$ . At 1.8  $m/s^2$ , no slip was observed and at 3.6  $m/s^2$  the TURTLE was clearly slipping and became hard to control. During the measurements, several sensors on the TURTLE were logged to determine whether slip has occurred. The precise procedure will be discussed later.

When slip occurs, the wheel's rotational velocity does not match its translational velocity anymore:  $\omega_w r_w \neq v_w$ . This property is also used for the definition of slip in Equation 1.2. The development of a difference between rotational velocity of the wheel with respect to its translational velocity, indicates that their accelerations do not match. As the wheel slips, it loses traction and resistance. The amount of force required to accelerate the slipping wheel thus drops.

So, three measurable phenomena exist that indicate slip:

**Speed** The rotational wheel speed does not match the translation wheel speed.

**Acceleration** The rotational wheel acceleration does not match the translation wheel acceleration.

**Motor effort** As the wheel slips, the loss of resistance allows the wheels to accelerate with less force.

As the motor effort for the wheels is determined by a complicated controller, the motor effort does not always drop as would be expected at the occurrence of slip. In fact, the motor effort usually increases greatly at slip. However, as this is not a clear relation and as it is not very consistent, using the change in motor effort is not useful for the detection of slip.

The acceleration is in itself a rather noisy signal when measured with accelerometers due to existing vibrations. The velocity on the other hand, provides a much smoother signal than the acceleration as disturbances are filtered out at integration. Still, the velocity can become increasingly unreliable over time due to a minimal error in the average of the acceleration. As accelerometers on the TURTLE were rotated and long measurements were done, the velocity indeed changes too much to give reliable results. In contrast, the noisy data of the acceleration measurements can be counteracted by a lot of filtering, thus making the data useful.

For these reasons, the acceleration method was used to detect slip.

### 4.2 Data acquisition

To detect slip, the rotational acceleration of the wheels is compared to the acceleration of the TURTLE. The wheel's rotational acceleration can be calculated from the wheel's encoder counts. The acceleration of the TURTLE is measured with 100 Hz by the accelerometer in the Xsens MTi-1 series IMU and by the separate accelerometer integrated in the TURTLE with

1000 Hz. The data from the IMU is however not yet available in the TURTLE's software. This data is therefore logged separately using MT Manager on an independent laptop via cable connection.

Via data logging on the TURTLE, the encoder counts of the three wheels are saved together with the time intervals, the accelerometer data and the current reference position. The last is used to determine the acceleration that the TURTLE tries to achieve and which resulted in slip.

Via MT Manager the translational and rotational acceleration are saved along with the rotational speed and accompanying time intervals.

### 4.3 Data analysis

The logged data is very noisy, especially that of the accelerometers. The wheels' acceleration is obtained through double differentiation of the encoder counts, resulting in a very noisy signal as well. This noise has to be filtered out. All filtering is done with moving average filters. To avoid phase shift between signals, about the same cut-off frequency of 5 Hz is used for all filtering. The occurring phase shift is assumed equal for all filtering. This phase shift is then compensated for to match the filtered signals to the non-filtered signals.

The cut-off frequency of 5 Hz is determined after a small study into the amplitudes of the frequencies in the signals. The signals were very low-frequent and noise started to occur from around 7 Hz as can be seen in Figure 4.1.

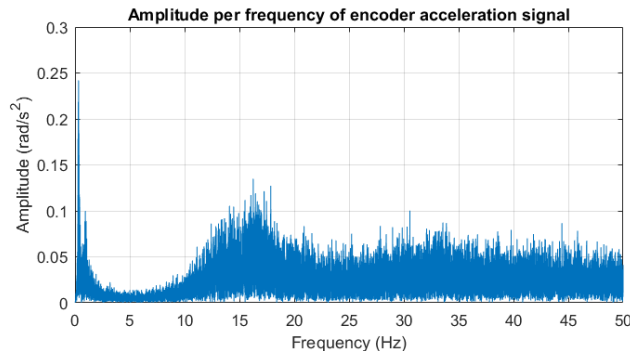


Figure 4.1: The frequency spectrum of the 2nd derivative of the wheel position as determined from the encoder counts.

The acceleration of the TURTLE is determined using the acceleration of the IMU as this data is less noisy in comparison with the integrated accelerometer. Additionally, the IMU also gives the angular acceleration, while the integrated accelerometer only provides linear acceleration. The data from the IMU and from the TURTLE are logged individually and are out of phase. In order to match the two datasets, the accelerometer data from the integrated accelerometer was down-sampled to 100 Hz to match the frequency of the IMU's signals. At the beginning of each measurement the TURTLE was given a firm push with both TURTLE and IMU recording. This acceleration peak was used to determine the phase shift between the two sets.

The IMU and the accelerometer are both rotated with respect to the coordinate system introduced in Figure 1.3. Firstly, the rotation of the integrated accelerometer is determined via fitting the velocity (calculated from integrating the acceleration) to the reference velocity. The accelerometer is not in the middle of the TURTLE, which means it also registers angular accelerations as linear accelerations. Therefore, this method is only valid for pure translational movement. As the accelerometer can be assumed fixed, previously determined values can be used for the rotation of the accelerometer.

Secondly, the rotation of the IMU is determined. This is done by fitting its velocity (from integration) to the velocity of the integrated accelerometer. As the acceleration of the IMU will be used for the determination of slip, purely linear acceleration of the TURTLE is needed, separated from the purely angular acceleration. The angular acceleration of the IMU is equal to the TURTLE's angular acceleration. The linear acceleration however, still needs modification. The measured linear acceleration of the IMU consists of the angular and linear acceleration of the TURTLE and the angular velocity as shown in Equation 4.1. The horizontal distance from the middle of the TURTLE to the IMU ( $R_{IMU}$ ) was first estimated using the 3D CAD model and was then improved during analysis until optimal results were received.

$$\vec{a}_{IMU} = \vec{a}_{TURTLE} + \vec{\alpha}_{TURTLE} \times R_{IMU} + \omega_{TURTLE} R_{IMU} \quad (4.1)$$

The three wheels A, B, C are checked for slip individually. This means that the acceleration and rotation of the TURTLE have to be converted to the linear acceleration of the wheels in their drive direction as specified by  $\vec{n}_i$  in Figure 1.3. This was done by use of the angle of the specific wheel ( $\psi_i$ ), the angle of acceleration ( $\psi_a$ ) and the distance from the wheel to the centre of the TURTLE ( $d_w$ ) as seen in Equation 4.2.

$$\vec{a}_i = \cos(\psi_i + \psi_a) a_{TURTLE} - d_w \alpha_{TURTLE} \quad (4.2)$$

The acceleration as determined by the encoders is compared to the acceleration as determined by the IMU. Slip is assumed to occur if the absolute acceleration of the encoders is  $2 \text{ m/s}^2$  larger than that according to the IMU for at least  $0.1 \text{ s}$ . These values were assumed as they provided the most optimal results, see also Chapter 6. When slip is detected, the reference acceleration that caused the slip is checked. The reference acceleration is used even though actual accelerations might vary, because the final goal is to limit the reference in order to avoid slip. The reference acceleration is determined through a double differentiation of the logged reference position and is a block signal. The causing acceleration is thus easily determined by searching for the maximum absolute value around the time at which slip occurs. This acceleration and the accompanying angle of acceleration are then stored.

#### 4.4 Slip occurrences

For the validation the TURTLE was accelerated manually in all directions with 10 degree intervals with accelerations ranging from  $1.8 \text{ m/s}$  to  $3.6 \text{ m/s}$ . Each acceleration/angle combination is executed about 5 times. In Section 4.3 is explained how this data is then converted to acceleration/angle pairs at which slip occurs. These stored acceleration and angle are plotted in Figures 4.2 - 4.5 in a similar manner as the model results. The color of the points indicates the amount of slip occurrences which have been detected at that acceleration/angle combination.

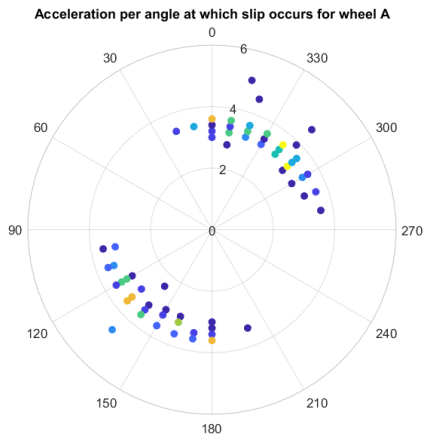


Figure 4.2: Detected number of slip occurrences per acceleration and angle at wheel A.

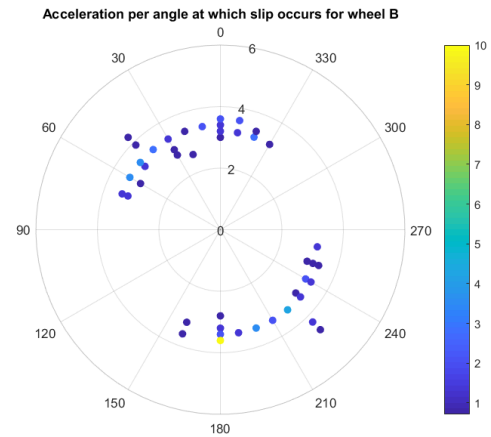


Figure 4.3: Detected number of slip occurrences per acceleration and angle at wheel B.

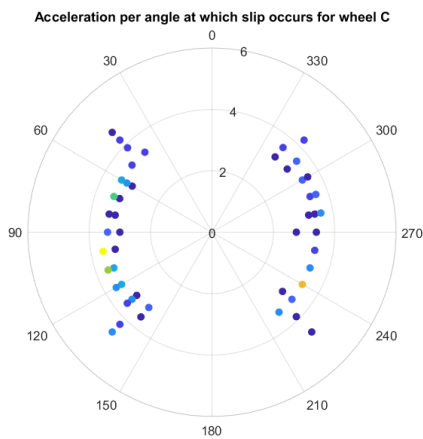


Figure 4.4: Detected number of slip occurrences per acceleration and angle at wheel C.

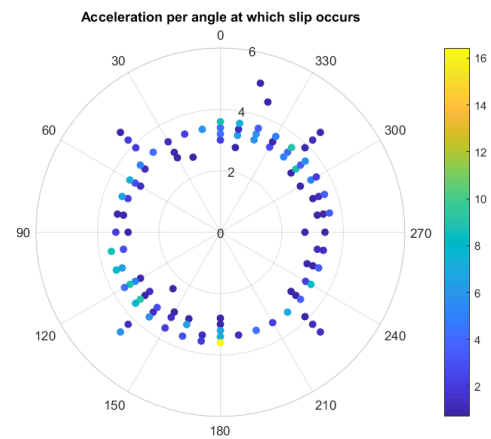


Figure 4.5: Detected number of slip occurrences per acceleration and angle at any of the wheels.

## 4.5 Comparison to model

It is clear to see that the model and the validation results do not match well. The distinct acceleration shape of the model does not show in the validation results. The validation results do not show a clear dependency of the maximal acceleration on the angles as is expected from the model. For easy comparison, the model and validation results are plotted together in Figure 4.6. For this, the friction factor of 0.5 is used although the friction factor is hard to determine due to the mismatch between model and measurements. Figure 4.6 is thus a combination of Figure 3.2 and 4.5.

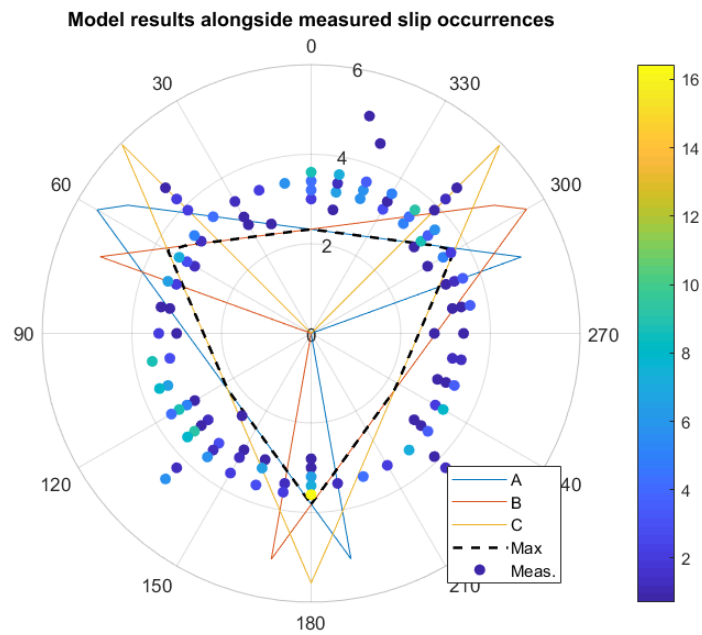


Figure 4.6: Measured slip occurrences together with modelled maximum acceleration with  $\mu = 0.5$ .

Although the model and the combined slip occurrences barely show any resemblance, the slip occurrences per wheel do match somewhat. Figures 4.2 - 4.4 do slip in approximately the same angle intervals as expected from the model. The shape per wheel however does not seem linear in the validation results. The non-slipping angle intervals also seem equally large, while the model shows a difference in these intervals, especially at larger values of friction factor  $\mu$ .

## 5 Conclusion

This report treats the research question: *How can the acceleration of the TURTLEs be improved?*

In order to be able to conclude on this research question several sub-questions were posed:

1. *What parameters influence the acceleration of the TURTLE and how?*
2. *What are the current values of these influencing parameters?*
3. *In what way can these parameters be changed to improve acceleration?*
4. *Can the TURTLE's acceleration be made dependent on its current state?*

In order to answer these questions, the current mechanical properties of the TURTLE are investigated (Chapter 2) and the maximum acceleration of the TURTLE is modelled (Chapters 1 & 3). It was then attempted to validate this model with practical measurements (Chapter 4). The sub-questions are answered below though their validity is questionable as the validation was unsuccessful. The influencing parameters and their values are stated in Table 5.1. Note that the significance is judged within realistic values for the TURTLE.

Table 5.1: Properties of the TURTLE as determined from the 3D model.

Parameter	Influence	Value
$m$ [kg]	None	36.0
COG [mm]	Insignificant	$[-3.46, 1.85, 165.59]^T$
$I_{zz}$ [kg m <sup>2</sup> ]	Insignificant	0.799
$\psi$ [rad]	Significant $\pm$	$0 \geq \psi \geq 2\pi$
$\mu$ [-]	Significant +	0.5
$k$ [rad/m]	Significant -	$k \in \mathbb{R}$

Although the inertias and COG can be changed without too much difficulty, their influence is insignificant. By increasing the friction factor through for example changing wheels, the acceleration can be increased greatly. The angle of acceleration and the amount of angular acceleration can be changed by smarter trajectory planning. This requires that the maximum acceleration as set in TURTLE's software should be made dependent on the  $\psi$  and  $k$ , which is possible, but not yet worked out.

## 6 Discussion

For answering the research question and the sub-questions, some assumptions were made and actions were taken that need some further discussion. The validity of these assumptions and actions are discussed below.

**Slip Condition** As mentioned in Chapter 1, the definition of slip, which was used for modelling, only distinguishes between slip and non-slip. In reality, slip is always present at rolling. The only distinction to be found is that between stable and unstable slip. The used slip-model is therefore perhaps too much of a simplification and not adequate.

**Speed dependence** The model only evaluates the force and moment equilibrium, independent of speed. During the validation, it appeared that when accelerating at higher speeds, slip was more clearly visible. Although this might appear as the TURTLE accelerates longer and slip is present longer, more research into the influence of speed is advisable.

**Simultaneous slip** The model calculates the maximum acceleration before slip occurs, while the validation looks at various accelerations until slip occurs. When one of the wheels slips, this has an effect on the other wheels as well, because the applied force by the slipping wheel drops. This relation between different wheels is not incorporated in the model. At the validation it was often observed that wheels slipped simultaneously, which supports the theory that the wheel slip affects the other wheels. This results in unreliable results for the validation.

**Acceleration difference** Slip is detected in the measured data by comparing the acceleration of the wheel according to the encoders with that according to the IMU. When the encoders show a much higher acceleration, this interval is indicated to show slip. This difference between the two measured acceleration is set to at least  $2 \text{ m/s}^2$ , but this is a dubious value. It was expected that clear peaks arise when the slip becomes unstable, but a lot of peaks were visible and the value of  $2 \text{ m/s}^2$  required some imagination. It must be noted though, that other values were also tested and no clear correlation with the model was found either.

**Filtering** Using the acceleration method for the validation, the signals required extensive filtering before they were useful. Still, the most basic filtering has been used: moving average filtering. This may result in quite some loss of data. Better filters are advised, especially for the acceleration determined from the encoders. A promising technique which has been looked into is time-stamping [6], but because of time constraints, this was not applied.

**Slip correction** The goal of the report was to research how to improve the acceleration of the TURTLE. Throughout the report the maximum acceleration defined the acceleration at which the TURTLE was on the verge of slipping, but it might be able to accelerate faster and compensate for a small amount of slip. When the maximum acceleration without (unstable) slip is for example  $3 \text{ m/s}^2$ , the acceleration might be set to  $3.2 \text{ m/s}^2$  without any problems, as the controllers of the TURTLE correct for the slip.

## 6.1 Recommendations

Although the research question is answered and implementation in the software is already possible, the validity should be checked first, for both linear and angular accelerations. This can be done best by improving the filtering (e.g. time-stamping) and doing additional measurements with smaller acceleration intervals. If this still does not validate the model, the model might have to be adapted to use a more realistic, better slip model than presented in Chapter 1. [7]

Some relations are clear already, like the influence of the friction factor. A next step in increasing the maximum acceleration would be increasing the friction factor, by for example designing better wheels.

The relations of the maximum acceleration per wheel on the angle as discussed in Section 3.3 can be determined. A simple function for the depending on the angle will make the implementation considerably easier.

The model can also be extended for the new TURTLEs with more wheels, which are currently under development. It would certainly be interesting to see how much more agile these new TURTLEs are.

A final option is to skip modelling completely and go straight for the experimental maxima of the TURTLE's acceleration. Although experiments are most reliable, the maximum acceleration will have to be determined each time anything changes, like playing on a different field. Additionally, determining when unstable slip occurs from experimental data has proved to be quite difficult.

## References

- [1] Tech United Eindhoven.
- [2] RoboCup. RoboCup objective.
- [3] J.L. Meriam and L.G. Kraige. *Dynamics*. John Wiley & Sons, Inc., Singapore, 7th edition, 2013.
- [4] A W Van Zundert. Traction Control for Omni-directional Robots. 2011.
- [5] Mark W. Spong, Seth Hutchinson, and Vidyasagar M. Robot Modeling and Control. *Control*, 141(1):419, 2006.
- [6] R. J E Merry, M. J G van de Molengraft, and M. Steinbuch. Velocity and acceleration estimation for optical incremental encoders. *Mechatronics*, 20(1):20–26, 2010.
- [7] Robert L Williams II, Brian E Carter, Paolo Gallina, and Giulio Rosati. Dynamic Model with Slip for Wheeled Omni-Directional Robots. *IEEE TRANSACTIONS ON ROBOTICS AND AUTOMATION*, 18(3):285–293, 2002.

# Appendices

## A Centre of gravity influence

In this appendix, the influence of the position of the centre of gravity (COG) is evaluated. To determine the influence of the position, the x, y and z position are variated and treated separately. For each direction several friction factors are evaluated. Where one of the directions is evaluated, the other two directions are set to the reference value:  $COG_{ref} = [0, 0, 165]^T$

### A.1 Varying the height of the COG

For friction factors ranging from 0.3 to 0.6, the maximum acceleration was plotted for several heights. These heights are displayed in the legends of the plots in *mm*.

It can be seen that the influence of the height of the COG has an insignificant influence. From Figures A.5 and A.6, it can be seen that the influence becomes a lot bigger when tipping becomes limiting, though the influence still remains small. For a more detailed analysis on the influence of the height of the COG, see Section 3.3.

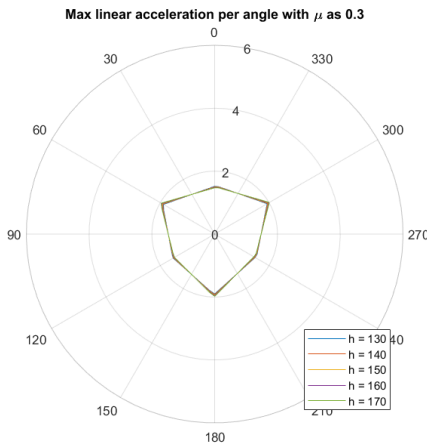


Figure A.1: Maximum acceleration per angle for different heights of the COG with a friction factor of 0.3.

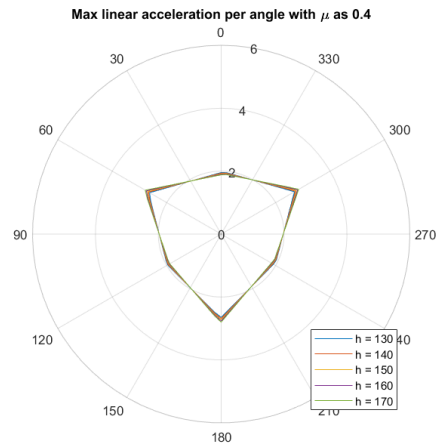


Figure A.2: Maximum acceleration per angle for different heights of the COG with a friction factor of 0.4.

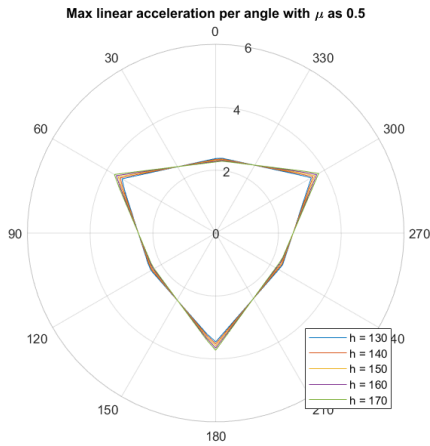


Figure A.3: Maximum acceleration per angle for different heights of the COG with a friction factor of 0.5.

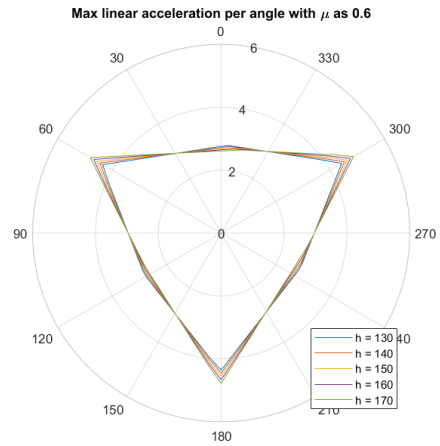


Figure A.4: Maximum acceleration per angle for different heights of the COG with a friction factor of 0.6.

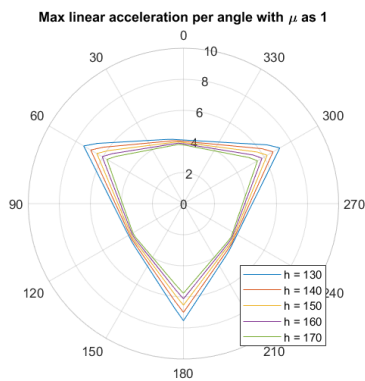


Figure A.5: Maximum acceleration per angle for different heights of the COG with a friction factor of 1.

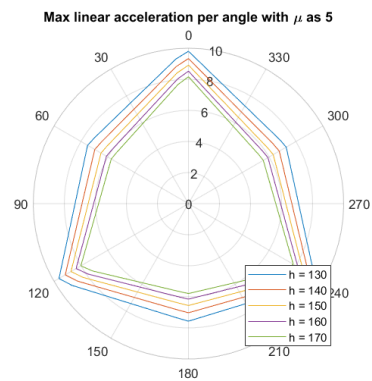


Figure A.6: Maximum acceleration per angle for different heights of the COG with a friction factor of 5.

## A.2 Varying the x-position of the COG

For friction factors ranging from 0.3 to 0.6, the maximum acceleration was plotted for several x-positions of the COG. These values of the x-coordinate of the COG are displayed in the legends of the plots in *mm*.

It can be seen that the influence of the x-position of the COG has a small influence. A clear difference can be seen between the maximum acceleration lines for the different x-coordinates, but these different x-positions vary 30 *mm*, which is quite much. Varying the x-coordinate is also beneficial for a certain range of angles and simultaneously disadvantageous for another range of angles. Changing the x-coordinate is therefore not deemed a good parameter for optimizing the TURTLE's acceleration.

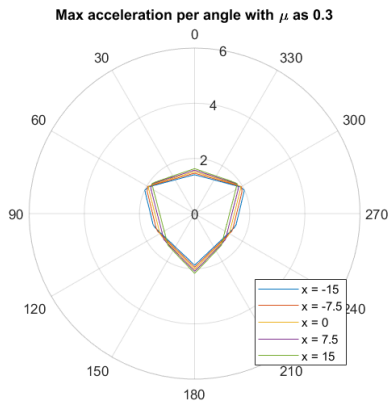


Figure A.7: Maximum acceleration per angle for different x-coordinates of the COG with a friction factor of 0.3.

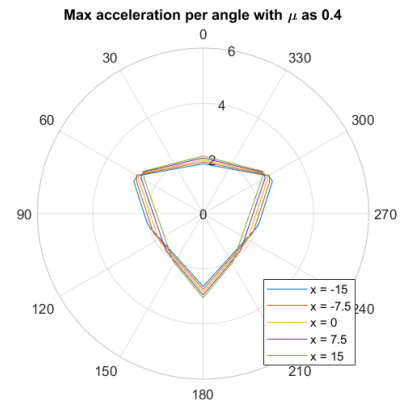


Figure A.8: Maximum acceleration per angle for different x-coordinates of the COG with a friction factor of 0.4.

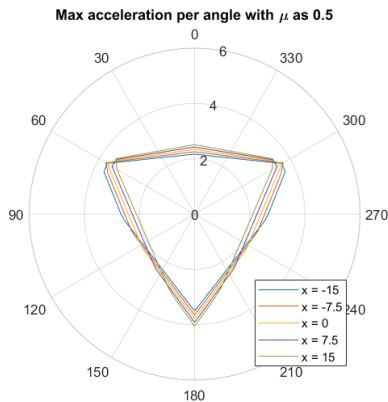


Figure A.9: Maximum acceleration per angle for different x-coordinates of the COG with a friction factor of 0.5.

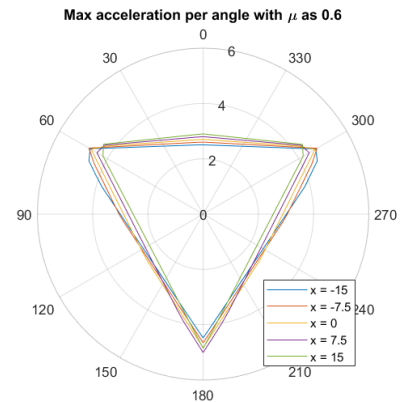


Figure A.10: Maximum acceleration per angle for different x-coordinates of the COG with a friction factor of 0.6.

### A.3 Varying the y-position of the COG

For friction factors ranging from 0.3 to 0.6, the maximum acceleration was plotted for several y-positions of the COG. These values of the y-coordinate of the COG are displayed in the legends of the plots in *mm*.

Analogous to varying the x-coordinate, the influence of the y-position of the COG has a small influence. A clear difference can be seen between the maximum acceleration lines for the different y-coordinates, but these different y-positions vary 30 *mm*, which is quite much. Changing the y-coordinate is beneficial for a certain range of angles and simultaneously disadvantageous for another range of angles. Changing the y-coordinate is therefore not deemed a good parameter for optimizing the TURTLE's acceleration.

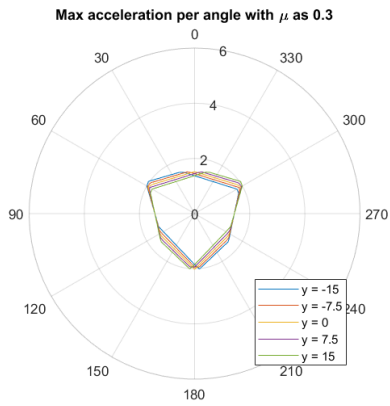


Figure A.11: Maximum acceleration per angle for different  $y$ -coordinates of the COG with a friction factor of 0.3.

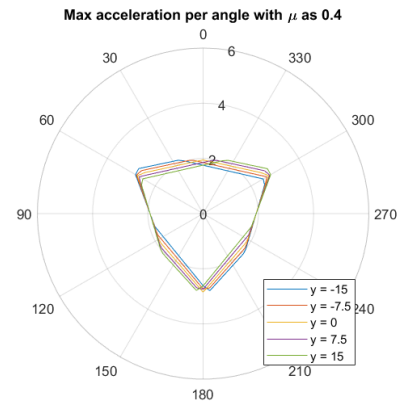


Figure A.12: Maximum acceleration per angle for different  $y$ -coordinates of the COG with a friction factor of 0.4.

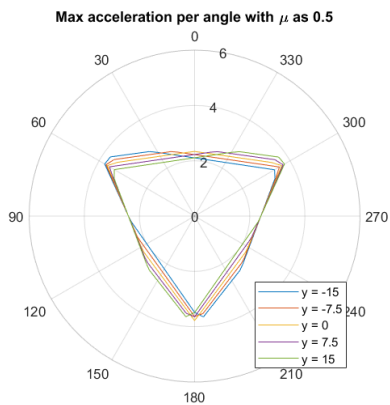


Figure A.13: Maximum acceleration per angle for different  $y$ -coordinates of the COG with a friction factor of 0.5.

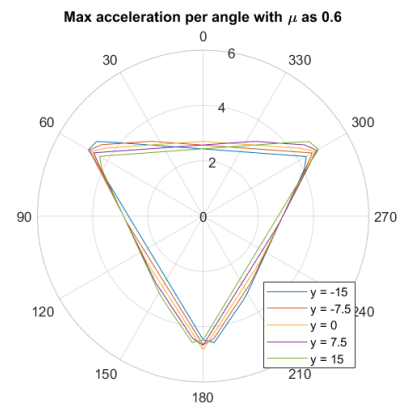


Figure A.14: Maximum acceleration per angle for different  $y$ -coordinates of the COG with a friction factor of 0.6.

## B Mass influence

Using the reference values of the TURTLE from Chapter 2, the maximum acceleration was evaluated for several masses of the TURTLE. These masses are indicated in the legends of the plots in  $kg$ .

In Figures B.1 and B.2 the maximum acceleration for four different masses is plotted. The Figures show there exists no dependence on the mass at all. This can be explained by the fact that both acceleration and gravitational force both depend on the mass linearly. These two influences by the mass are therefore cancelled out.

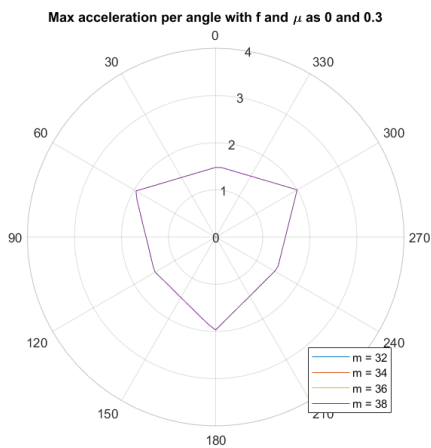


Figure B.1: Maximum acceleration per angle for different masses with a friction factor of 0.3.

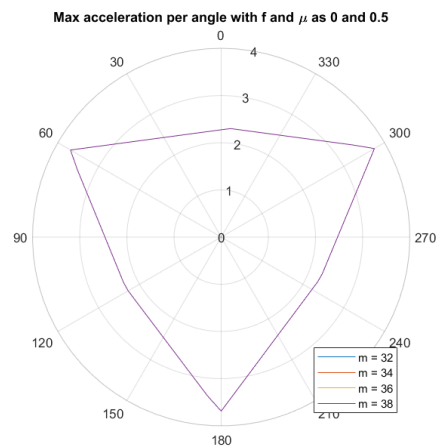


Figure B.2: Maximum acceleration per angle for different masses with a friction factor of 0.5.

## C Moment of inertia influence

Using the reference values of the TURTLE from Chapter 2, the maximum acceleration was evaluated for several moments of inertia of the TURTLE. These moments of inertia are indicated in the legends of the plots in  $kg\ m^2$ . As the moment of inertia clearly only has an influence when angular acceleration is involved,  $k$  was changed as well, just as the friction factor.

From Figures C.1 and C.2, it can easily be concluded that the friction factor still has a large influence. Furthermore, the moment of inertia seems to influence the maximal acceleration considerably. The influence of the moment of inertia also increases relatively at larger values of  $k$  (Figures C.2 and C.4. However, the range taken for the moment of inertia is rather large. Within reasonable parameters for the moment of inertia, it has an insignificant influence.

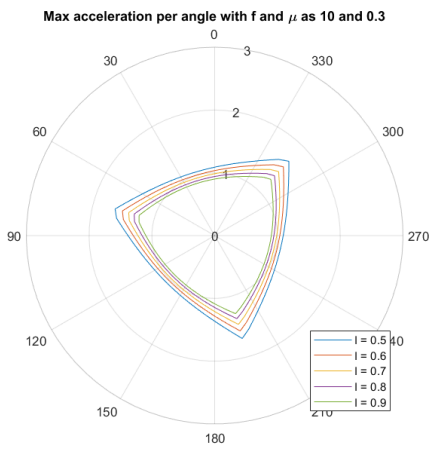


Figure C.1: Maximum acceleration per angle for different moment of inertia with  $k$  as 10 and a friction factor of 0.3.

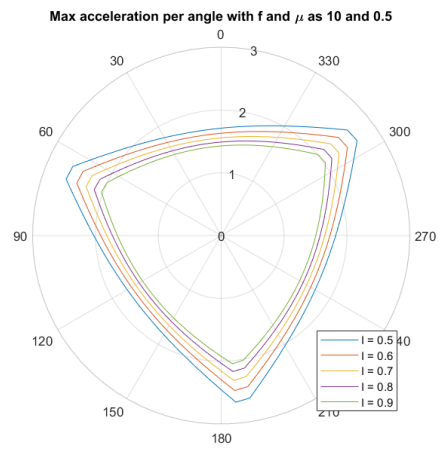


Figure C.2: Maximum acceleration per angle for different moment of inertia with  $k$  as 10 and a friction factor of 0.5.

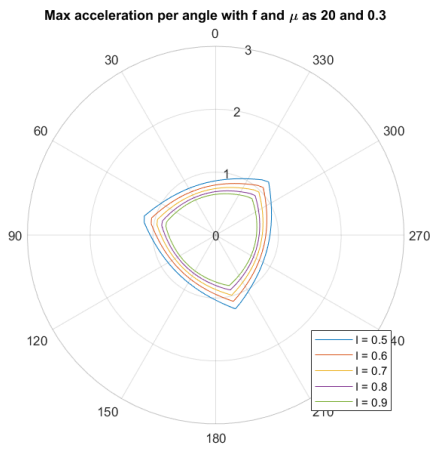


Figure C.3: Maximum acceleration per angle for different moment of inertia with  $k$  as 20 and a friction factor of 0.3.

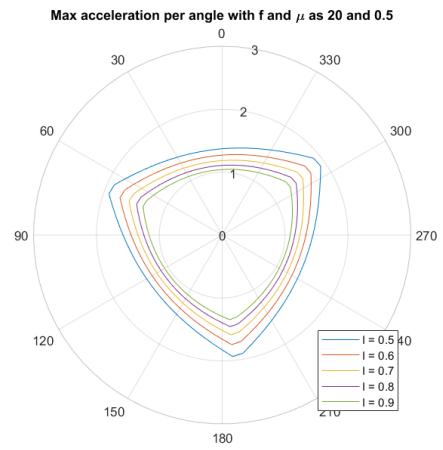


Figure C.4: Maximum acceleration per angle for different moment of inertia with  $k$  as 20 and a friction factor of 0.5.